Synthesis, chemical characterization, and biological evaluation of a novel auranofin derivative as an anticancer agent

Damiano Cirri,[a] Lara Massai,[b] Chiara Giacomelli,[c] Maria Letizia Trincavelli,[c] Annalisa Guerri,[b] Chiara Gabbiani,[a] Luigi Messori*[b] and Alessandro Pratesi*[a]

A novel gold(I) complex inspired by the known medicinal inorganic compounds auranofin and thimerosal, namely ethylthiosalicylate(triethylphosphine)gold(I) (AFETT hereafter), was synthesized and characterised and its structure solved through X-ray diffraction. The solution behavior of AFETT, its interactions with two biologically relevant proteins (i.e. human serum albumin and haemoglobin), and with a synthetic dodecapeptide reproducing the C-terminal portion of thioredoxin reductase, were comparatively analyzed through ^{31}P NMR and ESI-MS. Remarkable binding properties toward these biomolecules were disclosed. Moreover, the cytotoxic effects produced by AFETT on two ovarian cancer cell lines (A2780 and A2780R) and one colorectal cancer cell line were measured and found to be strong and nearly superimposable to those of auranofin. Interestingly, for both compounds, the ability to induce downregulation of vimentin expression in A2780R cells was evidenced. Despite its close similarity to auranofin, AFETT is reported to exhibit some peculiar and distinctive features such as lower lipophilicity, increased water solubility and faster reactivity towards the selected target biomolecules. These differences might confer to AFETT significant pharmaceutical and therapeutic advantages over auranofin itself.

1. Introduction

The use of metal-based compounds for medical purposes has a very ancient origin. For instance, it is known that antimony compounds were already used by the Egyptians as topic antiparasitic ointments.[1] In a closer period, spread from the 16th to 19th century, other metal compounds have been employed for treating many diseases. For example, some mercury and bismuth-based compounds were historically used for the treatment of syphilis,[2] whereas the gold(I) complex potassium dicyanoaurate was proposed by Robert Koch for the treatment of tuberculosis.[3] In the 20th century, with the advent of modern organic chemistry, metal-based drugs treatments were gradually abandoned, principally due to the severe side effects often associated with their usage. Anyway, some relevant examples of metal-based drugs are still present in the actual clinical protocols. This is, of course, the case of platinum compounds in the treatment of cancer,[4] as well as the employment of arsenic trioxide against promyelocytic leukaemia.[5] Other leading examples are thimerosal (a mercury-based and FDA-approved antiseptic)[6] and the clinically established gold-based antirheumatic compounds such as sodium aurothiomalate and auranofin (AF).[7] Notably, due to the advent and success of the drug repurposing approach,[8] many auranofin-related compounds have been investigated for the treatment of tumoral and parasitic diseases, sometimes with encouraging results.[9–11] In this frame, we have synthesized a new auranofin derivative in which the thiosugar moiety is replaced by an ethyl thiosalicylate ligand. The choice of a thiosalicylate derivative ligand was justified by its well-known anti-inflammatory properties[12] as well as its structural affinity with benzisothiazolinone, a widely reported antimicrobial agent.[13] Moreover, a thiosalicylate moiety can be found in the molecular structure of the thimerosal itself. In other words, we have designed a novel gold(I) drug candidate inspired by two clinically established metal-based drugs, i.e. auranofin and thimerosal (Fig. 1).

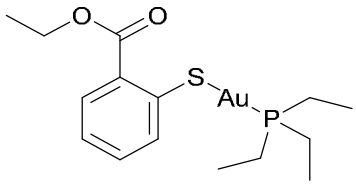

Fig. 1 Molecular structure of the investigated compound.

This novel compound, namely ethylthiosalicylate (triethylphosphine) gold(I) (AFETT hereafter), has been characterized in detail from the chemical point of view and its structure solved through single-crystal X-ray diffraction. Its reactivity against representative biological molecular targets (such as HSA and the TrxR synthetic dodecapeptide) was assessed through ^{31}P NMR and ESI-MS experiments. Moreover, the antiproliferative effects of the new compound were tested on human ovarian and colorectal cancer cell lines demonstrating its ability to induce cell apoptosis and the blockade of the cell cycle.

[a] *Department of Chemistry and Industrial Chemistry (DCCI), University of Pisa, Via Giuseppe Moruzzi 13, 56124 Pisa, Italy. E-mail: alessandro.pratesi@unipi.it*
[b] *Department of Chemistry "Ugo Schiff", University of Florence, Via della Lastruccia 3-13, 50019 Sesto Fiorentino, FI, Italy. E-mail: luigi.messori@unifi.it*
[c] *Department of Pharmacy, University of Pisa, Via Bonanno 6, Pisa 56126, Italy.*
Electronic Supplementary Information (ESI) available: NMR characterization, ^{31}P NMR spectra for solution stability studies, crystal data and refinement parameters, ^{31}P NMR spectra for biomolecules interaction studies and additional cellular experiments. See DOI: 10.1039/x0xx00000x

2. Results and Discussion

2.1. X-ray structure

During the first synthesis attempts, some crystals suitable for X-ray diffraction were obtained leaving a flask containing a hexane/chloroform solution of the product to stand for one week at -20 °C. The X-ray analysis showed that the asymmetric unit contains one molecule of the title complex. The metal atom has the typical linear coordination, the bond lengths of the gold(I) (Table S1) are in the range found for similar complexes retrieved in the CSD (v. 5.42 November 2020).[14] Interestingly, the crystallographic structure shows the peculiar direct interaction between the Au(I) centre of one AFETT molecule and the gold atom of another adjacent molecule. The Au-Au bond length is 3.0112(4) Å with the symmetry operation -x+1, -y+1, z (Fig. 2). This dimer is repeated throughout all the crystal. This feature has already been found in similar compounds published by us.[10] Crystal data and refinement parameters are reported in Table S2. CCDC contains the supplementary crystallographic data for this paper (deposition number: 2142915). These data can be obtained free of charge from the Cambridge Crystallographic Data Centre via http://www.ccdc.cam.ac.uk/Community/Requestastructure.

2.2. Solution behaviour and LogP evaluation

The chemical stability of AFETT was studied under strong coordinating conditions through ^{31}P NMR spectroscopy. More precisely, the complex stability was monitored up to 72 h in DMSO-d_6 solution and in DMSO-d_6/H_2O solution.

In all the recorded spectra, the ^{31}P NMR signal belonging to AFETT remains substantially unmodified during the selected timeframe. However, it is worthy of note that already in the first spectrum recorded at t_o a new and very small peak is present beside the one of AFETT. This signal is present both in the case of DMSO-d_6 and DMSO-d_6/H_2O solutions and remains stable in intensity for at least up to 72 h. According to the data already reported for similar gold(I) complexes,[9,11] this new signal can be reasonably attributed to phosphorus in the cationic monocharged complex $[Au(PEt_3)_2]^+$, which is likely due to the AFETT ligands scrambling equilibrium in solution through rearrangement, according to the equilibrium reported in Fig. 3 (see figures S4-S7 in supporting material). Despite the very low amount of the rearranged products, to the best of our knowledge, the biological effects of $[Au(Thiosalicylate)_2]^-$ anion have not been investigated. Conversely, the activity of $[Au(PEt_3)_2]^+$ has already been reported in is very similar to that of AF.[15,16]

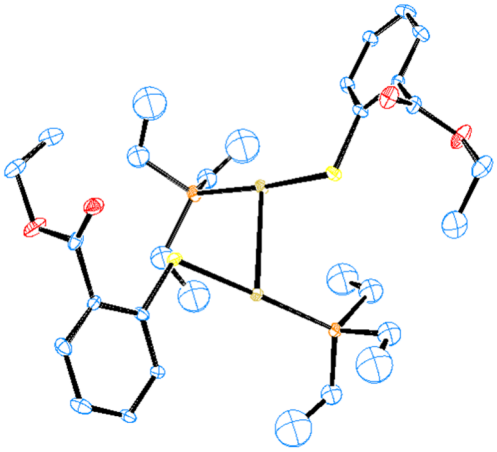

Fig.2. Crystal structure of AFETT.

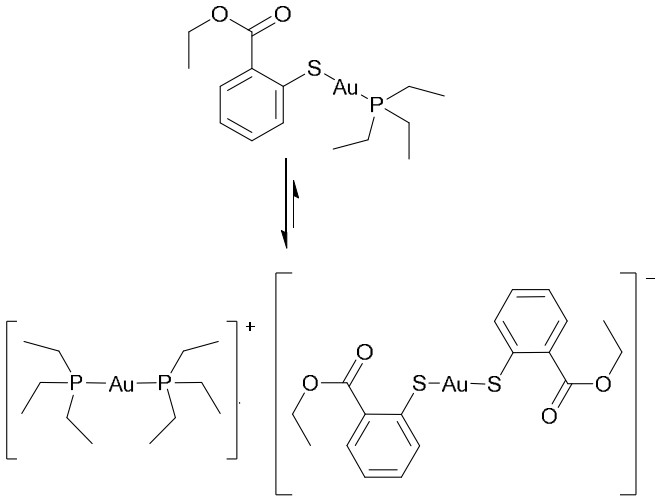

Fig. 3 Ligand rearrangement equilibrium for AFETT.

Furthermore, since the lipophilicity of a complex represents an important parameter strictly correlated with the cellular uptake, the partition coefficients log $P_{O/W}$ were determined via ICP-OES measurements and are reported in Table 1. The results obtained indicate a slight improvement of the hydrophilic character of AFETT with respect to AF.

Moreover, in order to further elucidate the in-solution behaviour of AFETT in comparison to the parent compound AF, we evaluated the water solubility by means of ^1H NMR spectroscopy.[17] In accordance with the LogP value found, AFETT turned out to possess a water solubility about twofold with respect to AF (Table 1). Those results mean that AFETT maintains a sufficient lipophilicity degree for the crossing of the cellular membrane associated with improved water solubility.[18] Hence, AFETT shows large stability in strongly coordinating solutions and a suitable lipophilic character that makes this compound an ideal candidate for further biological testing.

Table 1. Solubility in D_2O at 30 °C (^1H NMR, Me_2SO_2 internal standard) and octanol-water partition coefficients at 30 °C (Log $P_{O/W}$, ICP-OES).

Compound	Water solubility (mmol L^{-1})	Log $P_{O/W}$
Auranofin	0.12	1.6[a]
AFETT	0.24	0.9

[a] Log $P_{O/W}$ value already published.[6,9]

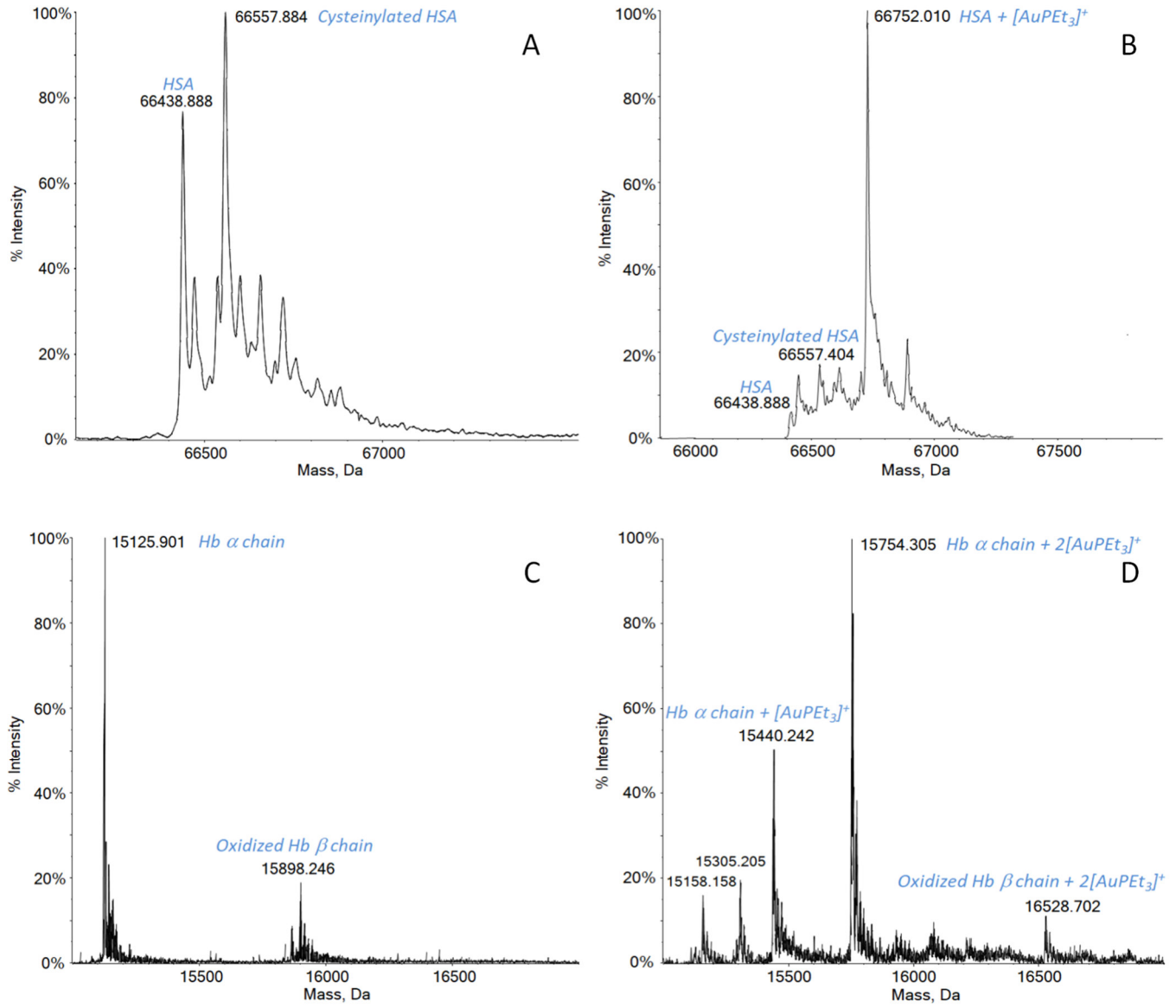

Fig. 4 Deconvoluted mass spectra recorded 2 mM ammonium acetate solution, pH 6.8 for: (A) HSA 5 × 10^{-7} M; (B) AFETT incubated with HSA at 37 °C for 24 h in 1:3 protein-to-gold ratio; (C) Hb 5 × 10^{-7} M; (D) AFETT incubated with Hb at 37 °C for 4 h in 1:3 protein-to-gold ratio. In all samples was added 0.1% v/v of formic acid before infusion into the mass spectrometer.

2.3. Biological targets selection

The reactivity of AFETT towards a few possible biological targets was investigated through ^{31}P NMR spectroscopy and ESI mass spectrometry. The selected biological targets were human serum albumin (HSA), haemoglobin (Hb), and a synthetic thioredoxin reductase fragment containing the Sec-Cys redox-active motif (namely, dTrxR (488-199)). Among all the possible biological targets, HSA represents the most abundant mammalian protein in the plasma, with a concentration of about 0.3 mM. Moreover, it is widely studied for its propensity to interact with gold-based compounds, especially through the unique free cysteine residue (Cys34).[19,20] Another relevant transport protein in the bloodstream is represented by haemoglobin. Also in this case, the protein is endowed with a solvent-accessible free cysteine residue able to rapidly interact with the Au(I) centres.[20] Lastly, since the gold compounds are extensively studied as potent inhibitors for the mitochondrial thioredoxin reductase (TrxR), an important and ubiquitous flavoenzyme critically involved in the regulation of intracellular redox metabolism, targeting TrxR has been regarded as a promising strategy for cancer drug development.[21–23] However, the TrxR is commercially available only in amounts suitable for the enzymatic assay but not compatible with the ESI-MS analysis. In this frame, we decided to challenge AFETT with a synthetic dodecapeptide reproducing the C-terminal tryptic fragment of the TrxR and bearing the peculiar -Cys-Sec- reactive motif (i.e. dTrxR (488-199)).[24,25] This peptide has been already adopted by our group as an alternative model for the TrxR reactivity.[26]

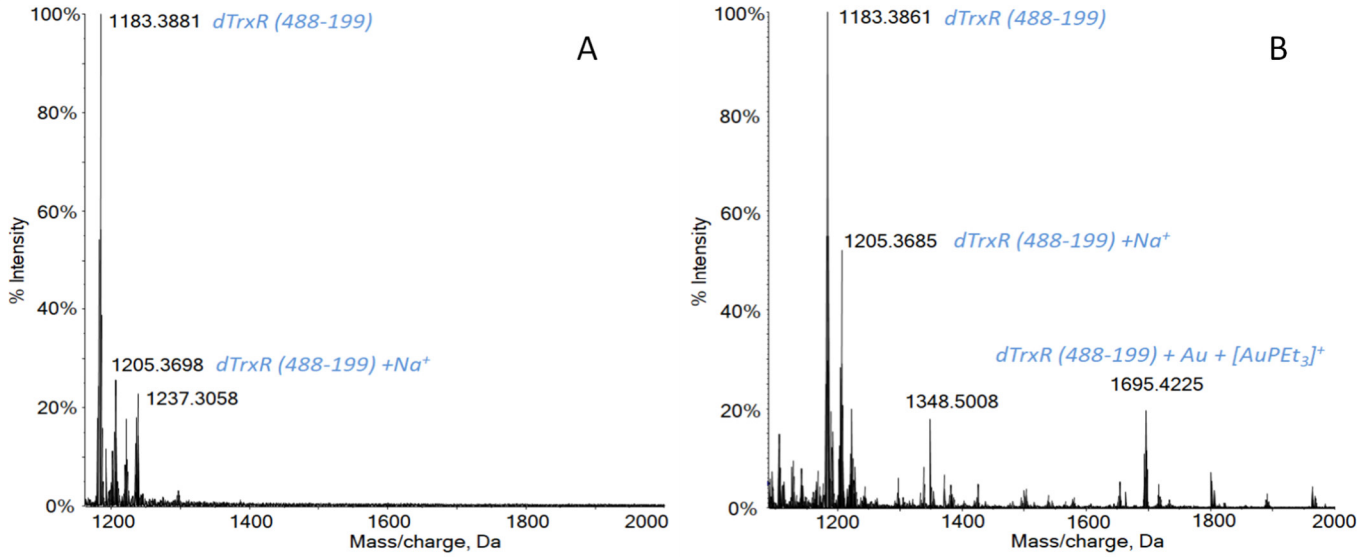

Fig. 5 (A) ESI mass spectrum of dTrxR (488-199) 5 × 10^{-7} M in 2 mM ammonium acetate solution, pH 6.8; (B) AFETT incubated with dTrxR (488-199) in 2 mM ammonium acetate solution, pH 6.8, in a 1:3:5 peptide-to-gold-to-DTT ratio. 0.1% v/v of formic acid was added just before infusion.

2.4. ^{31}P NMR experiments

The interaction of AFETT with human serum albumin (HSA) gave birth to four different peaks at t_0, attributable to triethylphosphine oxide (δ = 65 ppm), probably formed from the reduction of HSA disulfide bonds; to $[Au(PEt_3)_2]^+$ cation (δ = 47.3 ppm), formed through the equilibrium described in fig. 3; to unreacted AFETT (δ = 39.2 ppm); and to phosphate anion (δ = 2.3 ppm), which reasonably originated from the hydrolysis of phosphine oxide. The experiment was then repeated on the same sample after 24 h of incubation at 37 °C. In this case, three peaks were detected and assignable again to triethylphosphine oxide (δ = 65 ppm); to a classical HSA-AFETT adduct, in which the $[Au(PEt_3)]^+$ moiety of AFETT was bound to the free thiol group belonging to Cys34 of the HSA amino acid sequence (δ = 39.5 ppm); and to the previously listed phosphate anion (δ = 2.3 ppm). The spectra are reported in the supporting material (figures S8-S9). These results seem to confirm a reactivity pattern very close to that shown by auranofin itself.[27]

A similar experiment was conducted on the thioredoxin reductase dodecapeptide dTrxR (488-199) (see figures S10-S11 in supporting material). In this case, the presence of an interaction between AFETT and the peptide was immediately detectable (δ = 56.7 ppm) together with unreacted AFETT (δ = 39.2 ppm). After 24 h of incubation at 37 °C, AFETT turned out to be completely disappeared, since in the spectrum are present only the signal due to the interaction with the peptide (δ = 56.7 ppm) together with a tiny peak most probably attributable to the interaction of AFETT with 1,4-dithiothreitol used for the reduction of the intramolecular S-Se bond in the peptide (δ = 39 ppm).

Moreover, with the same technique, we tried also to investigate the reactivity of AFETT with human haemoglobin. Unfortunately, with the lyophilized protein at our disposal was not possible to obtain aqueous solutions with the necessary protein concentration for the ^{31}P NMR experiments. Nonetheless, a few NMR studies were also previously reported by Frank Shaw for the interaction between Hb directly extracted from red blood cells and very similar gold(I) compounds (i.e. auranofin and $[Au(PEt_3)Cl]$). The results provided definitive evidence for gold binding at the protein via the Cys-β-93 thiol groups, which are on the surface of the β subunits and solvent-exposed.[28]

2.5. ESI-MS experiments

The reactions of AFETT with the proteins HSA and Hb and with the peptide dTrxR (488-199) were also investigated by ESI-MS measurements.

The interactions of these proteins/peptide with AFETT were investigated according to a standard experimental setup including: preparation of a protein solution in 2 mM ammonium acetate at pH 6.8; addition of a triple excess of AFETT; incubation for 4 and 24 hours at 37 °C. The ESI mass spectra for both incubation times were subsequently recorded.[29,30]

Interpretation of these spectra is quite straightforward. In all cases, AFETT-protein adducts are formed as evidenced by the appearance of new peaks with greater masses characterized by a mass shift of +315 Da. This mass increase well matches with the mass of an $[Au(PEt_3)]^+$ fragment in line with previous observations with auranofin.[20]

The interaction of the gold complex with human serum albumin and haemoglobin was proved by ESI-MS analysis. The results obtained reacting HSA with AFETT in a 1:3 protein-to-metal ratio are reported below in comparison to the ESI mass spectrum of HSA (Fig. 4A and 4B). Two main signals are detected: one at 66438 Da assigned to the native protein, and another at 66558 Da due to the Cys34 cysteinylation.[26,31] Upon addition of 3 equivalents of AFETT an almost complete metallation of the albumin is detected after 24h, as evidenced by an intense peak at 66752 Da corresponding to the binding between HSA and the $[Au(PEt_3)]^+$ metal fragment. Since gold(I) compounds are highly thiophilic, we might assume that the

Cys34 residue could be a preferential binding site for the gold(I) fragments, as already demonstrated for auranofin. Figures 4C and 4D show the mass spectra of haemoglobin and of the same protein incubated for 4 h at 37 °C with AFETT, respectively. Again, the signals of the unreacted protein (15126 Da for the Hb α-chain, and 15898 Da for the oxidised Hb β-chain) are entirely replaced with those of the new adducts formed. Worthy of note, the almost complete haemoglobin metallation occurred in a few hours. In fact, in fig. 4D are shown three different signals at greater masses; namely, at 15440 and 15754 Da are present the signals of the mono and the bis adduct, respectively, of the aforementioned $[Au(PEt_3)]^+$ fragment with the Hb α-chain. Moreover, the oxidised form of the Hb β-chain reacts giving rise to an adduct bearing two copies of the gold(I) cationic fragment.

Given that the thioredoxin reductase enzyme is considered one of the major targets for cytotoxic gold compounds, the C-terminal dodecapeptide mimicking the TrxR1 active site was selected as a reliable model to study the reactivity of this gold(I) complex toward the thioredoxin reductase enzyme.[24,26]

The peptide possesses the reactive -Cys-Sec- motif as a possible binding site, the amino acid sidechains of these two residues form an intramolecular -S-Se- bridge which must be reduced to restore the original reactivity of the -Cys-Sec- TrxR motif. So, the reducing agent dithiothreitol (DTT) was added in 5:1 DTT/peptide ratio 30 minutes before the incubation of the dodecapeptide with the gold complex. The mass/charge spectrum in Fig. 5A shows the characteristic signals of the peptide and of its adducts with Na^+ and K^+ ions that are normally present in the solution. Upon reaction with the gold complex, the common trend of reactivity was confirmed: besides the unreacted peptide signal, a new signal was recorded indicating the binding of the $[Au(PEt_3)]^+$ fragment with the peptide. In addition, in this case the adduct is also characterized by the presence of an additional Au(I) ion deprived of the PEt_3 ligand. A further experiment was performed to compare the reactivity and the interactions which occur with HSA and AFETT or AF; specifically, the spectra of the two complexes with albumin

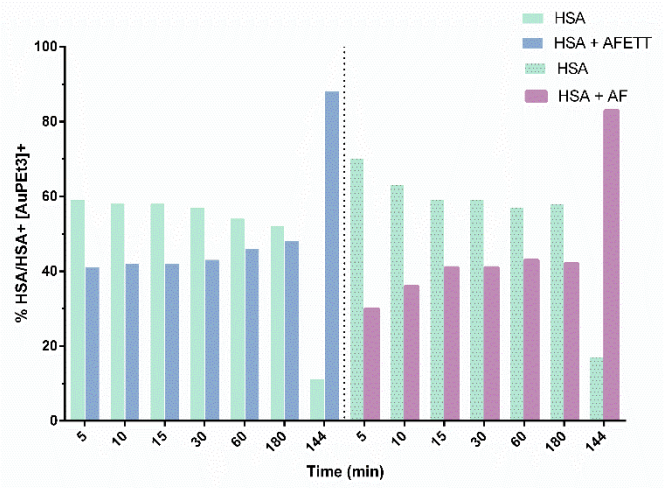

Fig. 6 The percentage ratio between free HSA and HSA metallated by AFETT (on the left) and the percentage ratio between free HSA and HSA metallated by AF (on the right).

were recorded at 5, 10, 15, 30 minutes and at 1, 3 and 24 hours. Interestingly, AFETT is somewhat kinetically faster than auranofin, within the first few minutes as shown in Fig. 6.

Hence, from the analysis of the data gathered through the interaction studies with the selected proteins, AFETT proved to be a highly reactive compound towards the tested biomolecules, inducing almost a complete metalation for both albumin and haemoglobin already in a very short timeframe (4 h).

2.6. *In vitro* evaluations

Evaluation of TrxR inhibition. The selenoprotein TrxR is recognized as a primary target of auranofin.[21] Thus, the inhibitory effects of AFETT on TrxR activity were evaluated in the A2780 cells extract. IC_{50} values (nM) were determined by treating 25 µg of cell lysate with increasing concentration of the compounds (0.1 nM - 5 µM) (Table 2). AF showed an IC_{50} value of 20.13 nM, in accordance with literature data.[15] Interestingly, AFETT demonstrated a slightly better ability to inhibit TrxR with and IC_{50} values of 16.86 nM. Overall, the results demonstrate that AFETT has a similar mechanism of action to AF, suggesting an anti-proliferative effect on cancer cells.

Table 2. IC_{50} values (nM) of TrxR inhibition determined for auranofin and AFETT. A2780 (25 µg) were incubated for 5 min with increasing concentration of the compounds (0,1 nM-5 µM), the increase of absorbance was monitored at 412 nm from 10 min to 1h.

Cell line	auranofin[a]	AFETT[a]
A2780	20.13 ± 2.50	16.86 ± 1.80

a Results are reported as the mean ± SD of two independent experiments.

Evaluation of cytotoxic activity. The anti-proliferative activity of AF against different types of cancer has been widely reported.[32,33] Among the others, AF decreases the growth of ovarian cancer cells.[34] Herein, the effects of the new compound AFETT were first evaluated on A2780 cells and their cisplatin-resistant counterpart (A2780 R) (Table 3). The activity of AFETT was compared to AF. After 72 h of exposure, AF (100 nM–10 µM) significantly decreased the proliferation of A2780 cells yielding an IC_{50} value of 0.98 ± 0.16 µM in accordance with previous literature data.[35] AFETT was able to decrease the A2780 cancer cell growth to a similar extent (IC_{50} 0.82 ± 0.13 µM). Interestingly, AF and AFETT were effective also against the A2780 R cells exhibiting an IC_{50} of 2.85 ± 1.13 µM and 3.04 ± 0.68 µM, respectively. The potent antitumor activity of auranofin has been reported also against colorectal cancer cells,[9] thus, the effects of AF and AFETT on HCT116 cells were evaluated (Table 3). AF was able to decrease the HCT116 viability with an IC_{50} of 0.83 ± 0.27 µM, in accordance with

Table 3. IC_{50} Values (µM) determined for Auranofin and AFETT

Cell line	Auranofin[a]	AFETT[a]
A2780	0.98 ± 0.16	0.82 ± 0.13
A2780 R	2.85 ± 1.13	3.04 ± 0.68
HCT-116	0.83 ± 0.27	0.77 ± 0.25
hGF	2.15 ± 0.41	1.64 ± 0.47

[a] Results are reported as the mean ± SD of three independent experiments.

literature data.[36,37] Interestingly, the new compound AFETT was able to reduce the HCT116 cell growth with similar potency (IC_{50} of 0.77 ± 0.25 μM). To assess the new compound selectivity for cancerous cells with respect to healthy cells, the gold complexes were also screened for their anti-proliferative effects on human fibroblast cells (hGF, Table 3). As evidence, AF and AFETT inhibited the cell growth of fibroblast with IC_{50} values of 2.15 ± 0.41 μM and 1.64 ± 0.47 μM, respectively. Interestingly, the activity against the healthy cells was significantly lower with respect to the ovarian and colorectal cancer cells.

Evaluation of apoptosis induction and cell cycle blockade. The anti-proliferative effects can be ascribed to the activation of different phenomena. Thus, to deeply investigate the mechanisms of action of this new golden derivative, the ability of AFETT to induce apoptosis and to perturb the cell cycle progression was investigated (Fig. 7 and Fig. S12, S13). The A2780 and A2780-R cells were treated with AF and AFETT (1 μM) for 48 h. AF was able to significantly reduce the A2780 cells in G1/G0 phase and a concomitant increase of cells in the G2/M phase highlighting its ability to induce a cell cycle blockade in G2/M (Fig. 7A). Interestingly, a similar effect was evidenced also in the cisplatin-resistant cells. These effects are in accordance with the ability of auranofin to block the cell cycle of small lung cancer cells in G2/M phase.[38] The new gold compound AFETT produced similar effects on both A2780 and A2780-R cells (Fig. 7A, B). Specifically, it increased the number of G1/G0 cells increasing the number of G2/M cells in both sensitive and resistant cells. Taken together, these results demonstrate the ability of the new complex to reduce the cell viability through a cell cycle perturbation similar to the effects prompted by auranofin attesting also the compound's ability to overcome cisplatin resistance.

Then, the type of cell death induced by AFETT in comparison with AF was better investigated. A2780 and A2780-R cells were treated with AFETT and AF (1 μM) for 48 h (Fig. 7C, D). AF and AFETT caused a significant phosphatidylserine externalization, both in the absence (early apoptosis) and presence of 7-aminoactinomycin D (7-AAD) staining (late apoptosis/death; Fig. 7C). The amount of total apoptotic cells was lower in cisplatin-resistant cells with respect to the sensitive ones, in accordance with the lower effect of both gold complexes on A2780-R cell viability (Table 2).

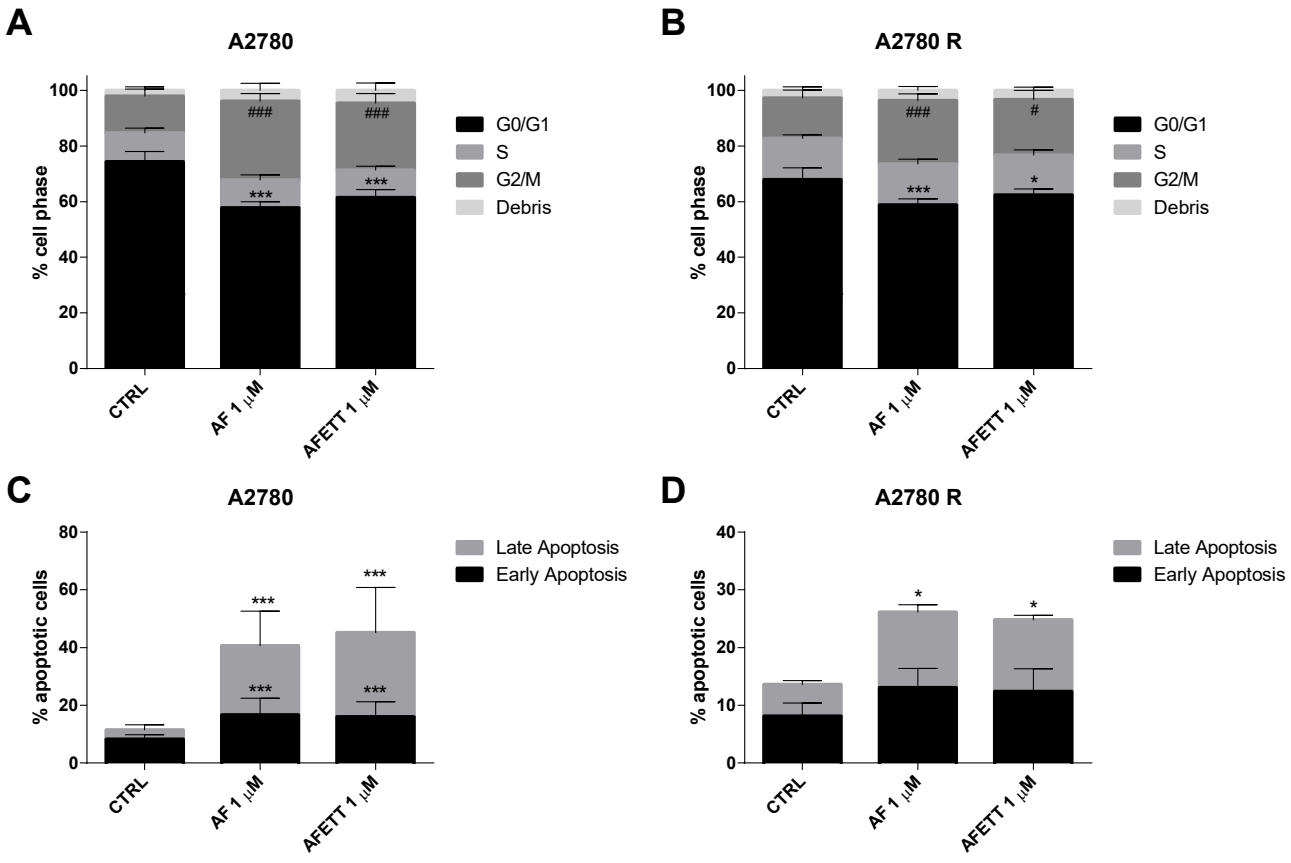

Fig. 7 A2780 (A, C) and A2780-R (B, D) cells were treated with AU and AFETT for 48 h. After incubation time, (A, B) the cell cycle distribution or (C, D) apoptosis induction were evaluated. (A, B) Data are expressed as the percentage of cells in the different phases (G0/G1, S, or G2/M) versus total cell number. Data represent the mean ± SD of three different independent experiments. The statistical significance of the differences was determined with a one-way ANOVA with Bonferroni post-test: *p<0.05, ***p<0.001 vs G0/G1 cells of the CTRL; # p<0.05, ### p<0.001 vs G2/M cells of the CTRL. (C, D) The apoptosis was quantified using Annexin V staining. The data are expressed as the percentage of apoptotic cells versus the total number of cells. Data represent the mean ± SD of three different independent experiments. The statistical significance of the differences was determined with a one-way ANOVA with Bonferroni post-test: *p<0.05, ***p<0.001 vs respective early or late apoptosis of the CTRL.

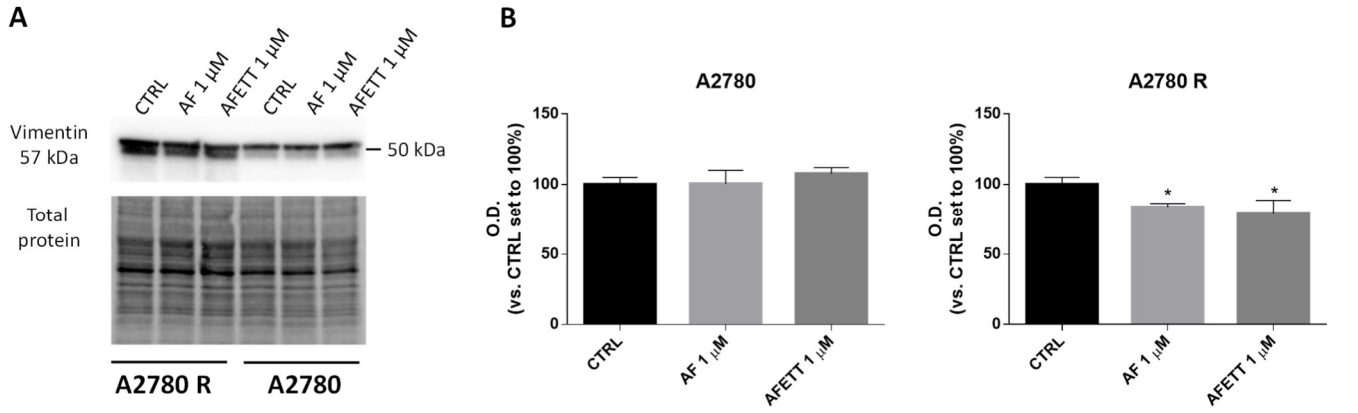

Fig. 8 A2780 and A2780-R cells were treated with AU and AFETT (1 μM) for 48 h. After the incubation time, the vimentin expression was quantified by western blot analysis. (A) A representative image of vimentin immunoblot and total protein. (B) The densitometric analysis of western blot image. Data are expressed as percentages versus the CTRL set to 100% and represent the mean ± SD of three different independent experiments. The statistical significance of the differences was determined with a one-way ANOVA with Bonferroni post-test: *p<0.05 vs CTRL.

Evaluation of vimentin expression in response to AFETT. The aggressiveness of different types of cancer has been linked to different mechanisms including the epithelial-mesenchymal transition (EMT). The cell conversion from an epithelial phenotype to a mesenchymal one increases ovarian cancer cell invasiveness and enhances their degree of malignancy.[39–41] The major molecular determinants of EMT are the downregulation of epithelial cell markers, E-cadherin and ß-catenin, and up-regulation of the mesenchymal markers, vimentin and N-cadherin.[42–44] Herein, to elucidate the effects of gold complexes on EMT induction, the modulation of vimentin expression was evaluated (Fig. 8A, B). A2780 and A2780-R cells were treated with AF and AFETT (1 μM) for 48 h and the vimentin protein expression was evaluated by Western blot analysis. The vimentin expression in A2780 cells was not significantly affected by AF or AFETT treatment. Interestingly, challenging the A2780-R cells with AF and AFETT caused a significant decrease in vimentin expression highlighting the ability of these gold complexes to reduce the aggressiveness of resistant ovarian cancer cells.

3. Conclusions

The search for new and more effective metal-based anticancer agents able to overcome the severe drawbacks of cisplatin represents, to date, one of the main challenges for the bioinorganic chemists' community.[45,46] Several studies have been carried out, also by these authors, on metal-based compounds containing different metal centres.[17,47–49] Among a large number of alternatives proposed, gold-based compounds cover a principal role in the new potential anticancer agents scenario.[50] The gold(I) complex auranofin is the leading experimental anticancer agent of the family of gold-based drugs and is currently undergoing a few clinical trials.[51] Accordingly, this has triggered renewed attention for this kind of compounds, and in particular for a few AF-related complexes previously prepared and characterized.[27] Some of these authors have also been involved in a systematic study of AF and of their related complexes bearing the $[Au(PEt_3)]^+$ reactive moiety. In particular, we focused our attention on the synthesis and biological characterization of new Au(I) compounds where the thiosugar ligand of AF is replaced by an halido ligand.[9,10,52,53] Interestingly, these complexes showed better antiproliferative properties with respect to AF towards the reference cancer cell line A2780 and also towards the colorectal cancer cell line with negligible cytotoxic effects on healthy cells.[9,10]

Now, we have presented here a new AF derivative where the tioglucosetetraacetate ligand is replaced with an ethylthiosalicylate molecule (AFETT). The new compound has been fully characterized, showing good stability in physiological-like conditions. Moreover, the reactivity studies with some putative target biomolecules like the human serum albumin, haemoglobin and a synthetic dodecapeptide mimetic of the human thioredoxin reductase have been performed. In the case of the two proteins, AFETT showed a high degree of metallation, even at very short incubation times (i.e. 5 min). Furthermore, from the direct comparison with the same data obtained for AF, a somewhat faster kinetics of the reaction was clearly evidenced for AFETT. The maintained reactivity of this new compound for the TrxR dodecapetide was also a crucial feature, pointing out to a preserved inhibitory activity for the thioredoxin reductase, being one of the main recognised modes of action for gold-based compounds.[23,54]

Replacement of the thiosugar ligand with the ethylthiosalicylate ligand resulted in increased stability in aqueous solutions and enhanced reactivity of AFETT for the selected biomolecules. Those behaviours could be due also to the more hydrophilic character of the complex with respect to AF, as suggested by the LogP values of 0.9 and 1.6, respectively.

In the light of these considerations, AFETT turned out to be in full agreement with the Lipinski's "rule of five" which identifies the five key physicochemical parameters (molecular weight,

lipophilicity, polar surface area, hydrogen bonding, and charge) required for a rational design of a bioactive metallodrug.[18]

In spite of the structural modification, it is of paramount importance to highlight the high antiproliferative activity of AFETT against the ovarian cancer cell lines (sensitive and resistant to cisplatin). In particular, the IC_{50} values obtained are almost superimposable to those obtained for AF, falling in both cases in the low micromolar range. Additionally, both compounds showed the ability to induce downregulation of vimentin expression in A2780R cells, proving the potential of these gold complexes to reduce the aggressiveness of cisplatin-resistant cancer cells.

Hence, on the basis of studies here reported, AFETT manifested all the required features to be considered as a new promising gold-based anticancer agent, deserving more in-depth pharmacological studies.

4. Experimental

4.1. Materials

All chemicals have been purchased from Carlo Erba, Sigma-Aldrich and Fluka and used without further purifications.

Lyophilized human haemoglobin (Hb) and human serum albumin (HSA) were purchased from Merck and used without further purification or manipulation, whilst the dodecapeptide of thioredoxin reductase (dTrxR (488-199)) was synthesized in the MetMed laboratories at the Department of Chemistry, University of Florence following already established procedures.[24,25] Dithiothreitol (DTT) and dimethyl sulfoxide (DMSO) were purchased from Fluka. LC-MS materials (water, methanol and ammonium acetate) were purchased from VWR and Honeywell.

4.2. Synthesis

Synthesis of ethyl thiosalicylate. Ethyl thiosalicylate was prepared through the classical Fischer esterification process starting from salicylic acid.[55] More in detail, 1 g of thiosalicylic acid was suspended in 40 mL of absolute ethanol. Subsequently, 5 mL of concentrated sulfuric acid (98%) were added dropwise to the reaction mixture. The formed solution was refluxed for 72 h with a bubble condenser equipped with a $CaCl_2$ stopper. After cooling the reaction mixture, 150 mL of 0.1 M ammonia were carefully added. The formed liquid/liquid suspension was extracted with chloroform (3 × 30 mL) and the recovered organic phase was washed with brine and dried with sodium sulfate. Subsequently, the suspension was filtered and the solvent was removed through a rotary evaporator. The crude product was obtained in quantitative yield and subsequently purified through flash column chromatography with a mixture of petroleum ether/chloroform 2:1 as eluent. The purified product was recovered as 910 mg of pale oil (yield 77 %). Its ^{1}HNMR spectrum was found to be fully consistent with already reported literature.[56]

Synthesis of AFETT. The investigated compound was prepared through already established procedures.[57] More in detail, 40 mg of commercially available Au(PEt_3)Cl have been dissolved in 4 mL of methanol and 31 mg of ethyl thiosalicylate have been added together with 35 mg of $NaHCO_3$ and the suspension stirred for 4 h. Subsequently, the solvent was removed through a rotary evaporator and the solid mixture suspended in chloroform. The suspension was filtered for removing the insoluble salts, then the solvent was removed under reduced pressure. The crude product appears as a yellow oil, that has been solubilized in 0.5 mL of chloroform. Subsequently, 10 mL of hexane have been added for inducing the precipitation of the purified product. The suspension was left to stand at -20 °C for 24 h, then filtered on a Hirsch funnel. The purified product was recovered as 46 mg of a yellowish crystalline solid (yield 81 %). ^{1}HNMR ($CDCl_3$; 400.13 MHz) δ: 7.85 (d, 1H, *J* = 7.84 Hz); 7.54 (d, 1H, *J* = 7.64 Hz); 7.12 (m, 1H); 7.00 (m, 1H); 4.40 (q, 2H, *J* = 7.12 Hz); 1.86 (dq, 6H, *J* (P-H) = 9.62 Hz, *J* (H-H) = 7.68 Hz), 1.41 (t, 3H, *J* = 7.12 Hz); 1.22 (dt, 9H, *J* (P-H) = 18.39 Hz, *J* (H-H) = 7.66 Hz). ^{13}CNMR ($CDCl_3$; 100.61 MHz) δ: 168.96; 142.62; 135.87; 134.62; 129.42; 129.22; 123.30; 60.84; 18.28 (d, *J* (P-H) = 33.04 Hz); 14.39; 8.98. ^{31}P NMR ($CDCl_3$; 161.97 MHz) δ: 36.57. Elemental analysis: Calc. [C: 36.30 %; H: 4.87 %; S: 6.46 %]; Exp. [C: 35.95 %; H: 4.32 %; S: 6.87 %]. HR-ESI-MS: $[M]^+$ *m/z* = 497.09720 (theoretical for $[C_{15}H_{24}AuO_2PS + H]^+$: *m/z* = 497.09730; error: -0.2 ppm).

4.3. X-ray diffraction

X-ray data collection was performed with a Bruker D8 Venture equipped with IμS 3.0 Microfocus Incoatec Source and a Photon III Detector. The Mo Kα radiation was used for the data collection performed at a temperature of 100 K, controlled by a CryoStream 700 (Oxford Cryosystems). Data were collected with the APEX II suite and refined and reduced with the program SAINT (SAINT V8.38A, Bruker AXS Inc., 2017). Absorption correction was achieved through the SADABS 2016/2,[58] included in the Bruker Package of data treatment. The structure was solved with the Shelxt Program and refined with Shelxl[59] by full-matrix least-squares techniques with anisotropic displacement parameters for all non-hydrogen atoms. The hydrogen atoms in the compound under investigation were introduced in calculated positions and refined considering a riding model with isotropic thermal parameters. All calculations were performed by using the program PARST,[60] implemented in the Crystal Structure crystallographic software package WINGX,[61] and molecular plots were produced with Mercury (v 2020.3.0).[62]

4.4. Measurement of lipophilicity (LogP)

The octanol-water partition coefficient was determined by a modified shake-flask method.[9] Water (250 mL, distilled after Milli-Q purification) and n-octanol (250 mL) were shaken together for 72 h to allow saturation of both phases in a 500 mL flask. The suspension was allowed to separate at least for one week in the dark. A solution of the complex was prepared using the water phase (1 mM) and an equal volume of octanol was added. Biphasic solutions were mixed for ten minutes and then centrifuged at 25 °C for 5 min at 6000 rpm to allow separation. Concentrations in both phases were determined through ICP-AES, following a well-established mineralisation protocol.[63]

Reported logP value is defined as log_{10}([complex]oct/[complex]wat). The final value was reported as the mean of three determinations.

4.5. Solubility determination

5 mg of the selected gold(I) complex was suspended in an Eppendorf test tube with 300 µL of D_2O and 300 µL of a Me_2SO_2/D_2O solution (Me_2SO_2 final conc. 6.37 mM). The suspension was heated to 30 °C and sonicated for 90 minutes. The resulting saturated solution was decanted, transferred to an NMR tube and then analysed through quantitative ^{1}HNMR spectroscopy (tilt angle = 45°; recycle delay = 4 s; number of scans = 12). The concentration (solubility) was calculated by the relative integral (related to phosphine -CH_3 groups) with respect to Me_2SO_2 (δ = 3.14 ppm).

4.6. NMR spectroscopy

NMR spectra were recorded in a Bruker Avance III 400 spectrometer equipped with a Bruker Ultrashield 400 Plus superconducting magnet (resonating frequencies: 400.13, 161.97, 100.61 MHz for ^{1}H, ^{31}P and ^{13}C, respectively) and a 5 mm PABBO BB-1H/D Z-GRD Z108618/0049 probe. Unless otherwise indicated, all the experiments were run at room temperature (25 ± 2 °C). Samples used in ^{31}P NMR experiments have been prepared as follows:

HSA interaction: 30 mg of HSA were dissolved in 435 µL of D_2O inside an Eppendorf tube, then 15 µL of a 30 mM DMSO solution of AFETT were added and the mixture shacked for 30 seconds. After, the mixture was moved to the NMR tube. The final concentration of the sample was 1 mM for both HSA and gold complex.

dTrxR (488-199) interaction: 3,87 mg of dTrxR (488-199), 2,4 mg of AFETT (1.5 eq) and 4.8 mg of 1,4-dithiothreitol (10 eq) were suspended in 300 µL of DMSO-d_6. Afterwards, 100 µL of ammonium acetate solution (20 mM; pH 6) were added to the suspension. The mixture was shacked and moved to the NMR tube.

4.7. ESI mass spectrometry

The ESI-MS investigations were performed using a TripleTOF® 5600$^+$ high-resolution mass spectrometer (Sciex, Framingham, MA, U.S.A.), equipped with a DuoSpray® interface operating with an ESI probe. All the ESI mass spectra were acquired through direct infusion at 7 µL/min flow rate. The general ESI source parameters optimized for each protein and peptide analysis were as follows:

HSA: positive polarity, ionspray voltage floating (ISFV) 5500 V, temperature (TEM) 25 °C, ion source gas 1 (GS1) 45 L/min; ion source gas 2 (GS2) 0 L/min; curtain gas (CUR) 12 L/min, collision energy (CE) 10 V; declustering potential (DP) 150 V, acquisition range 1000-2600 *m/z*.

Hb: positive polarity, ionspray voltage floating (ISFV) 5500 V, temperature (TEM) 25 °C, ion source gas 1 (GS1) 45 L/min; ion source gas 2 (GS2) 0 L/min; curtain gas (CUR) 12 L/min, collision energy (CE) 10 V; declustering potential (DP) 60 V, acquisition range 570-1300 *m/z*.

dTrxR (488-199): positive polarity, ionspray voltage floating (ISFV) 5500 V, temperature (TEM) 25 °C, ion source gas 1 (GS1) 25 L/min; ion source gas 2 (GS2) 0 L/min; curtain gas (CUR) 30 L/min, collision energy (CE) 10 V; declustering potential (DP) 300 V, acquisition range 1090-2000 *m/z*.

For acquisition, Analyst TF software 1.7.1 (Sciex) was used and deconvoluted spectra were obtained by using the Bio Tool Kit micro-application v.2.2 embedded in PeakView™ software v.2.2 (Sciex).

For the experiments with HSA and Hb, solutions of the protein 10^{-4} M and AFETT at a 1:3 protein-to-metal ratio were prepared diluting with ammonium acetate solution $2x10^{-3}$ M, pH 6.8. The mixtures were then incubated at 37 °C up to 24 h. For the experiments with dTrxR (488-199) peptide, a solution of the peptide 10^{-4} M was prepared diluting with ammonium acetate solution $2x10^{-3}$ M, pH 6.8. Then, aliquots of DTT stock solution were added in a 1:5 peptide-to-reducing agent ratio and the mixture was incubated for 30 minutes at 37 °C. Subsequently, an aliquot of AFETT solution was added in a 1:3 peptide-to-metal compound ratio. The mixture thus obtained was incubated at 37 °C up to 24 h.

After the incubation time, all solutions were sampled and diluted to a final biomolecule concentration of $5x10^{-7}$ M for HSA, Hb and dTrxR using ammonium acetate solution $2x10^{-3}$ M, pH 6.8. The final biomolecules solutions were also added with 0.1% v/v of formic acid just before the infusion in the mass spectrometer in order to enhance the ionization process.

The percentage of free and metallated HSA has been calculated according to the relative intensity of each peak *i.e.* free HSA, adduct HSA-AFETT, adduct HSA-AF.

4.8. Cellular studies

Cell culture. A2780 (Human ovarian carcinoma) and HCT116 cells (Human colorectal carcinoma cells) were kindly provided by Prof. Tania Gamberi, Department of Experimental and Clinical Biomedical Sciences "Mario Serio", University of Florence. A2780 R cells (Human ovarian carcinoma cisplatin-resistant) were kindly provided by Dr. Dario Puppi, Department of Chemistry and Industrial Chemistry, University of Pisa. Human gingival fibroblast cells (hGF) were purchased from CLS Cell Line Service GmbH (Germany), lot. number 300703-1541SF. A2780 and A2780 R cells were maintained in RPMI (Corning) supplemented with 10% FBS (Corning); HCT116 were maintained in DMEM-F12 (Corning) supplemented with 10% FBS (Corning) and hGF were maintained in DMEM-F12 (Corning) supplemented with 5% FBS (Corning). All the cell media were supplemented with 2 mM L-glutamine, 100 U/mL penicillin, and 100 µg/mL streptomycin and maintained at 37 °C in a humidified 5% CO_2 atmosphere.

Inhibition of TrxR enzymatic activity. The inhibition of TrxR enzymatic activity in cell lysates was performed as previously described.[15] Specifically, A2780 cells were cultured in P150; when a 90% confluence was reached, cells were washed with phosphate-buffered saline solution. Then, cells were scraped and homogenized with a Potter-Elvehjem homogenizer in 3 ml cold buffer (50 mM potassium phosphate, pH 7.4, 1 mM EDTA, containing a human protease inhibitor cocktail (Sigma). The

obtained lysate was centrifuge at 10.000 xg for 15 min at 4 °C and at the end, the pellet was discarded. The supernatant protein contents were determined with a Bradford Reagent (Biorad) using the bovine serum albumin as standard. 25 µg of proteins were used to assess the TrxR enzymatic assay. The TrxR inhibition was assessed using a commercial colorimetric assay kit (Cayman chemical, Item N° 10007892) based on the reduction of the 5,5'-dithiobis(2-nitrobenzoic) acid (DTNB) to 5-thio-2-nitrobenzoic acid (TNB) in the presence of NADPH, according to the manufacturer's instructions. The cell lysate was preincubated for 5 min with different concentrations of AF and AFETT. Then, the reaction was started with DTNB and monitored spectrophotometrically at 412 nm at different time points (10', 30', 1 h). The specific activity was evaluated using the inhibitor solution of mammalian TrxR present in the kit. The non-interference of the compounds with assay components was confirmed by negative control experiments without lysate solution. The IC_{50} value was calculated by measuring the percentage of inhibitor activity versus the control (specific activity of lysate alone) set to 100%. Data were fit using log(inhibitor) vs. normalized response -- Variable slope.

MTS assay. Cells were seeded in 96-well microplates (10.000 cells/well for A2780 and A2780R, 5.000 cells/well for HCT116 and hGF). After 24 h, cells were treated with concentrations ranging from 100 nM up to 10 µM of AF and AFETT for 72 h. Control was treated with DMSO alone to obtain a final concentration of 0.5%. Then, cell viability was determined using an MTS assay (CellTiter 96 AQueous One Solution Cell Proliferation Assay kit; Promega) according to the manufacturer's instructions. The absorbance values at 490 nm were measured with the Victor Wollac 2 multimode plate reader (Perkin Elmer).

Evaluation of cell cycle progression. A2780 and A2780 R were seeded in 6-well microplates (400.000 cells/well). After 24 h, the medium was replaced and cells were treated with DMSO (CTRL) or AF and AFETT for 48 h. The cell cycle progression was evaluated using Muse Cell Cycle Assay Kit (MCH100106) with the Muse Cell Analyzer (Merck KGaA), as previously described.[64]

Quantification of cell apoptosis. A2780 and A2780 R were seeded in 24-well microplates (100.000 cells/well). After 24 h, the medium was replaced and cells were treated with DMSO (CTRL) or AF and AFETT for 48 h. Muse Annexin V and Dead Cell Assay Kit (MCH100105) was used to stain the apoptotic cell population. The samples were analysed using the Muse Cell Analyzer instrument, as previously described.[64]

Western Blot analysis. A2780 and A2780 R cells were seeded in P60 petri dish (50.000 cells/cm^2). After 24 h medium was replaced and the cells were treated with DMSO (CTRL) or AF and AFETT (1 µM) for 48 h. At the end, cells were lysed with RIPA buffer. Thirty µg of total proteins were diluted in Laemmli solution, resolved by SDS-PAGE (4-20%), transferred to PVDF membranes and probed overnight at 4 °C with primary anti-Vimentin (diluted 1:1000, #5741; Cell Signaling Technology). The primary antibody was detected using appropriate anti-rabbit (diluted 1:10.00, A0545, Sigma Aldrich). The peroxidase was detected using a chemiluminescent substrate (ECL, Bio-Rad), and the images were acquired by ChemiDoc (Bio-Rad). Immunoreactive bands were quantified by performing a densitometric analysis with Image Lab (version 6.0.1; Bio-Rad Laboratories). Bands were normalized using total protein obtained with stain-free technologies.[65]

Statistical Analysis. Data were analysed using Graph-Pad Prism 6.0 (GraphPad Software Inc., San Diego, CA). The IC50 values were calculated using the "non-linear fit log(inhibitor) *vs*. normalized response -- Variable slope". Statistical analysis was performed as indicated in figure legends. A p-value of <0.05 was considered to be statistically significant.

Author Contributions

The manuscript was written through the contributions of all authors. All authors have given approval to the final version of the manuscript.

Conflicts of interest

There are no conflicts to declare.

Acknowledgements

The authors thank AIRC and Fondazione Cassa Risparmio Firenze for funding the project "Advanced mass spectrometry tools for cancer research: novel applications in proteomics, metabolomics and nanomedicine" (Multi-user Equipment Program 2016, grant number 19650). AP thanks the University of Pisa (Fondi di Ateneo 2020 and PRA_2020_39) and Beneficentia Stiftung (Vaduz, Liechtenstein, BEN2020/34) for the financial support. The CIRCMSB (Consorzio Interuniversitario di Ricerca in Chimica dei Metalli nei Sistemi Biologici, Italy) is also acknowledged. DC gratefully acknowledges Associazione Italiana per la Ricerca sul Cancro (AIRC) for financial support (two years fellowship for Italian project "Marcello e Rosina Soru"; project code: 23852).

Notes and references

1 H. Kamal, *Br. Med. J.*, 1926, **1**, 1102.
2 A. Gelpi and J. D. Tucker, *Sex. Transm. Infect.*, 2015, **91**, 68.1-68.
3 T. G. Benedek, *J. Hist. Med. Allied Sci.*, 2004, **59**, 50–89.
4 D. Wang and S. J. Lippard, *Nat. Rev. Drug Discov.*, 2005, **4**, 307–320.
5 D. Douer, W. Hu, S. Giralt, M. Lill and J. DiPersio, *Oncologist*, 2003, **8**, 132–140.
6 D. Cirri, M. G. Fabbrini, A. Pratesi, L. Ciofi, L. Massai, T. Marzo and L. Messori, *BioMetals*, 2019, **32**, 813–817.
7 A. E. Koch, M. Cho, J. Burrows, S. J. Leibovich and P. J. Polverini, *Biochem. Biophys. Res. Commun.*, 1988, **154**, 205–212.
8 D. Cirri, F. Bartoli, A. Pratesi, E. Baglini, E. Barresi and T. Marzo, *Biomedicines*, 2021, **9**, 504.
9 T. Marzo, D. Cirri, C. Gabbiani, T. Gamberi, F. Magherini, A. Pratesi, A. Guerri, T. Biver, F. Binacchi, M. Stefanini, A. Arcangeli and L. Messori, *ACS Med. Chem. Lett.*, 2017, **8**,

997–1001.
10 T. Marzo, L. Massai, A. Pratesi, M. Stefanini, D. Cirri, F. Magherini, M. Becatti, I. Landini, S. Nobili, E. Mini, O. Crociani, A. Arcangeli, S. Pillozzi, T. Gamberi and L. Messori, *ACS Med. Chem. Lett.*, 2019, **10**, 656–660.
11 T. Marzo, D. Cirri, S. Pollini, M. Prato, S. Fallani, M. I. Cassetta, A. Novelli, G. M. Rossolini and L. Messori, *ChemMedChem*, 2018, **13**, 2448–2454.
12 S. Côté, P. Carmichael, R. Verreault, J. Lindsay, J. Lefebvre and D. Laurin, *Alzheimer's Dement.*, 2012, **8**, 219–226.
13 V. Silva, C. Silva, P. Soares, E. M. Garrido, F. Borges and J. Garrido, *Molecules*, 2020, **25**, 991.
14 F. H. Allen, *Acta Crystallogr. Sect. B Struct. Sci.*, 2002, **58**, 380–388.
15 I. Landini, L. Massai, D. Cirri, T. Gamberi, P. Paoli, L. Messori, E. Mini and S. Nobili, *J. Inorg. Biochem.*, 2020, **208**, 111079.
16 D. Cirri, T. Schirmeister, E. J. Seo, T. Efferth, L. Massai, L. Messori and N. Micale, *Mol. 2020, Vol. 25, Page 4454*, 2020, **25**, 4454.
17 S. Braccini, G. Rizzi, L. Biancalana, A. Pratesi, S. Zacchini, G. Pampaloni, F. Chiellini and F. Marchetti, *Pharmaceutics*, 2021, **13**, 1158.
18 C. A. Lipinski, F. Lombardo, B. W. Dominy and P. J. Feeney, *Adv. Drug Deliv. Rev.*, 2001, **46**, 3–26.
19 A. Pratesi, D. Cirri, L. Ciofi and L. Messori, *Inorg. Chem.*, **57**, 10507–10510.
20 C. Zoppi, L. Messori and A. Pratesi, *Dalt. Trans.*, 2020, **49**, 5906–5913.
21 X. Zhang, K. Selvaraju, A. A. Saei, P. D'Arcy, R. A. Zubarev, E. S. Arnér and S. Linder, *Biochimie*, 2019, **162**, 46–54.
22 M. P. Rigobello, G. Scutari, A. Folda and A. Bindoli, *Biochem. Pharmacol.*, 2004, **67**, 689–696.
23 F. Magherini, T. Fiaschi, E. Valocchia, M. Becatti, A. Pratesi, T. Marzo, L. Massai, C. Gabbiani, I. Landini, S. Nobili, E. Mini, L. Messori, A. Modesti and T. Gamberi, *Oncotarget*, 2018, **9**, 28042–28068.
24 A. Pratesi, C. Gabbiani, E. Michelucci, M. Ginanneschi, A. M. Papini, R. Rubbiani, I. Ott and L. Messori, *J. Inorg. Biochem.*, 2014, **136**, 161–169.
25 A. Pratesi, C. Gabbiani, M. Ginanneschi and L. Messori, *Chem. Commun.*, 2010, **46**, 7001–7003.
26 L. Massai, C. Zoppi, D. Cirri, A. Pratesi and L. Messori, *Front. Chem.*, 2020, **8**, 1–14.
27 A. A. Isab, C. Frank Shaw, J. Lockela and J. D. Hoeschele, *Inorg. Chem.*, 1988, **27**, 3588–3592.
28 C. F. Shaw, M. T. Coffer, J. Klingbeil and C. K. Mirabelli, *J. Am. Chem. Soc.*, 1988, **110**, 729–734.
29 F. Sacco, M. Tarchi, G. Ferraro, A. Merlino, G. Facchetti, I. Rimoldi, L. Messori and L. Massai, *Int. J. Mol. Sci.*, 2021, **22**, 10551.
30 L. Massai, J. Fernández-Gallardo, A. Guerri, A. Arcangeli, S. Pillozzi, M. Contel and L. Messori, *Dalt. Trans.*, 2015, **44**, 11067–11076.
31 C. Zoppi, L. Massai, D. Cirri, C. Gabbiani, A. Pratesi and L. Messori, *Inorganica Chim. Acta*, 2021, **520**, 120297.
32 C. Yeo, K. Ooi and E. Tiekink, *Molecules*, 2018, **23**, 1410.
33 E. García-Moreno, A. Tomás, E. Atrián-Blasco, S. Gascón, E. Romanos, J. M. Rodriguez-Yoldi, E. Cerrada and M. Laguna, *Dalt. Trans.*, 2016, **45**, 2462–2475.
34 F. H. Abdalbari and C. M. Telleria, *Discov. Oncol.*, 2021, **12**, 42.
35 D. Cirri, I. Landini, L. Massai, E. Mini, F. Maestrelli and L. Messori, *Pharmaceutics*, 2021, **13**, 727.
36 A. A. Saei, H. Gullberg, P. Sabatier, C. M. Beusch, K. Johansson, B. Lundgren, P. I. Arvidsson, E. S. J. Arnér and R. A. Zubarev, *Redox Biol.*, 2020, **32**, 101491.
37 W. C. Stafford, X. Peng, M. H. Olofsson, X. Zhang, D. K. Luci, L. Lu, Q. Cheng, L. Trésaugues, T. S. Dexheimer, N. P. Coussens, M. Augsten, H.-S. M. Ahlzén, O. Orwar, A. Östman, S. Stone-Elander, D. J. Maloney, A. Jadhav, A. Simeonov, S. Linder and E. S. J. Arnér, *Sci. Transl. Med.*, 2018, **10**, eaaf7444.
38 X. Cui, S. Park and W. Park, *Oncol. Rep.*, 2020, **44**, 2715–2724.
39 D. Vergara, B. Merlot, J. P. Lucot, P. Collinet, D. Vinatier, I. Fournier and M. Salzet, *Cancer Lett.*, 2010, **291**, 59–66.
40 H. Yan and Y. Sun, *Oncol. Lett.*, 2014, **8**, 426–430.
41 N. Kenda Suster, S. Smrkolj and I. Virant-Klun, *J. Ovarian Res.*, 2017, **10**, 11.
42 J. Yang, P. Antin, G. Berx, C. Blanpain, T. Brabletz, M. Bronner, K. Campbell, A. Cano, J. Casanova, G. Christofori, S. Dedhar, R. Derynck, H. L. Ford, J. Fuxe, A. García de Herreros, G. J. Goodall, A. K. Hadjantonakis, R. J. Y. Huang, C. Kalcheim, R. Kalluri, Y. Kang, Y. Khew-Goodall, H. Levine, J. Liu, G. D. Longmore, S. A. Mani, J. Massagué, R. Mayor, D. McClay, K. E. Mostov, D. F. Newgreen, M. A. Nieto, A. Puisieux, R. Runyan, P. Savagner, B. Stanger, M. P. Stemmler, Y. Takahashi, M. Takeichi, E. Theveneau, J. P. Thiery, E. W. Thompson, R. A. Weinberg, E. D. Williams, J. Xing, B. P. Zhou and G. Sheng, *Nat. Rev. Mol. Cell Biol.*, 2020, **21**, 341–352.
43 C. Giacomelli, S. Daniele, L. Natali, C. Iofrida, G. Flamini, A. Braca, M. L. Trincavelli and C. Martini, *Sci. Rep.*, 2017, **7**, 15174.
44 S. Usman, N. H. Waseem, T. K. N. Nguyen, S. Mohsin, A. Jamal, M.-T. Teh and A. Waseem, *Cancers (Basel).*, 2021, **13**, 4985.
45 S. Manohar and N. Leung, *J. Nephrol.*, 2018, **31**, 15–25.
46 M. Hanif and C. G. Hartinger, *Future Med. Chem.*, 2018, **10**, 615–617.
47 G. Tamasi, A. Carpini, D. Valensin, L. Messori, A. Pratesi, F. Scaletti, M. Jakupec, B. Keppler and R. Cini, *Polyhedron*, 2014, **81**, 227–237.
48 L. Massai, A. Pratesi, J. Bogojeski, M. Banchini, S. Pillozzi, L. Messori and Ž. D. Bugarčić, *J. Inorg. Biochem.*, 2016, **165**, 1–6.
49 E. Barresi, I. Tolbatov, T. Marzo, E. Zappelli, A. Marrone, N. Re, A. Pratesi, C. Martini, S. Taliani, F. Da Settimo and D. La Mendola, *Dalt. Trans.*, 2021, **50**, 9643–9647.
50 C. Nardon, G. Boscutti and D. Fregona, in *Anticancer Research*, International Institute of Anticancer Research, 2014, vol. 34, pp. 487–492.
51 C. Roder and M. J. Thomson, *Drugs R D*, 2015, **15**, 13–20.

52 I. Tolbatov, D. Cirri, L. Marchetti, A. Marrone, C. Coletti, N. Re, D. La Mendola, L. Messori, T. Marzo, C. Gabbiani and A. Pratesi, *Front. Chem.*, 2020, **8**, 812.
53 A. Menconi, T. Marzo, L. Massai, A. Pratesi, M. Severi, G. Petroni, L. Antonuzzo, L. Messori, S. Pillozzi and D. Cirri, *BioMetals*, 2021, **34**, 867–879.
54 T. Gamberi, A. Pratesi, L. Messori and L. Massai, *Coord. Chem. Rev.*, 2021, **438**, 213905.
55 F. Viani, B. Rossi, W. Panzeri, L. Merlini, A. M. Martorana, A. Polissi and Y. M. Galante, *Tetrahedron*, 2017, **73**, 1745–1761.
56 C.-C. Chiang, T.-C. Chang, H.-J. Tsai and L.-Y. Hsu, *Chem. Pharm. Bull.*, 2008, **56**, 369–373.
57 D. Cirri, M. G. Fabbrini, L. Massai, S. Pillozzi, A. Guerri, A. Menconi, L. Messori, T. Marzo and A. Pratesi, *BioMetals*, 2019, **32**, 939–948.
58 L. Krause, R. Herbst-Irmer, G. M. Sheldrick and D. Stalke, *J. Appl. Crystallogr.*, 2015, **48**, 3–10.
59 G. M. Sheldrick, *Acta Crystallogr. Sect. C Struct. Chem.*, 2015, **71**, 3–8.
60 M. Nardelli, *J. Appl. Crystallogr.*, 1995, **28**, 659–659.
61 L. J. Farrugia, *J. Appl. Crystallogr.*, 2012, **45**, 849–854.
62 C. F. Macrae, I. Sovago, S. J. Cottrell, P. T. A. Galek, P. McCabe, E. Pidcock, M. Platings, G. P. Shields, J. S. Stevens, M. Towler and P. A. Wood, *J. Appl. Crystallogr.*, 2020, **53**, 226–235.
63 I. Landini, A. Lapucci, A. Pratesi, L. Massai, C. Napoli, G. Perrone, P. Pinzani, L. Messori, E. Mini and S. Nobili, *Oncotarget*, 2017, **8**, 96062–96078.
64 A. M. Iannuzzi, C. Giacomelli, M. De Leo, D. Pietrobono, F. Camangi, N. De Tommasi, C. Martini, M. L. Trincavelli and A. Braca, *J. Nat. Prod.*, 2020, **83**, 626–637.
65 R. L. S. Neris, A. M. C. Dobles and A. V. Gomes, in *Methods in molecular biology (Clifton, N.J.)*, 2021, vol. 2261, pp. 443–456.